Boundary-Layer Meteorol (2016) 159:173–181
DOI 10.1007/s10546-015-0106-9

NOTES AND COMMENTS

Planetary Boundary-Layer Modelling and Tall Building Design

Emil Simiu[1] · Liang Shi[1] · DongHun Yeo[1]

Received: 8 April 2015 / Accepted: 22 October 2015 / Published online: 12 November 2015

Abstract Characteristics of flow in the planetary boundary layer (PBL) strongly affect the design of tall structures. PBL modelling in building codes, based as it is on empirical data from the 1960s and 1970s, differs significantly from contemporary PBL models, which account for both "neutral" flows, and "conventionally neutral" flows. PBL heights estimated in these relatively sophisticated models are typically approximately half as large as those obtained using the classical asymptotic similarity approach, and are one order of magnitude larger than those specified in North American and Japanese building codes. A simple method is proposed for estimating the friction velocity and PBL height as functions of specified surface roughness and geostrophic wind speed. Based on published results, it is tentatively determined that, even at elevations as high as 800 m above the surface, the contribution to the resultant mean flow velocity of the component V normal to the surface stress is negligible and the veering angle is of the order of only 5°. This note aims to encourage dialogue between boundary-layer meteorologists and structural engineers.

Keywords Boundary-layer meteorology · Brunt–Väisälä frequency · Conventionally neutral stratification · Planetary boundary layer · Tall structures

1 Introduction

For structural engineering purposes, mean wind speeds in the turbulent planetary boundary layer (PBL) are currently modelled in North America and Japan by strictly empirical power laws developed essentially in the 1960s (Davenport 1965; Canadian Structural Design Manual 1971; AIJ recommendations for loads on buildings 2004; ASCE 7-10 Standard 2010). According to these models, wind speeds increase monotonically within the boundary layer up to the gradient height (the term "gradient height" being applied in such models to both

✉ Emil Simiu
emil.simiu@nist.gov

1 Engineering Laboratory, National Institute of Standards and Technology, Gaithersburg, MD 20899, USA

geostrophic and cyclostrophic winds), specified to be approximately 200–250 m above ground level for water surface exposures, 300–350 m for open terrain exposures, and 400–450 m for suburban terrain exposures. (The term "exposure" indicates that the surface roughness is uniform over a sufficiently long distance (the fetch) upwind of the structure of interest.) The power-law model further assumes that above the geostrophic height the flow is free of turbulence and the mean wind speed does not vary with height. Barotropic conditions are assumed.

Using asymptotic methods, the following results were obtained in the 1960s and 1970s: (1) the PBL height $H \approx 0.25u_*/f$ (u_* is the friction velocity, f is the Coriolis parameter) (e.g., Csanady 1967; Blackadar and Tennekes 1968; Tennekes 1973; Simiu and Scanlan 1996), that is, about one order of magnitude greater than given in the power-law model; (2) the mean flow in the PBL can be represented as a spiral structure, with components $U(z)$ and $V(z)$ parallel and normal to the surface stress, respectively; (3) the variation with height of the $U(z)$ component is logarithmic up to the geostrophic height H, i.e., $U(z) = (u_*/k)\ln(z/z_0)$ ($k \approx 0.41$ is the von Kármán constant, z_0 is the aerodynamic roughness length); (4) the component $V(z)$ is vanishingly small throughout the surface layer, the height of which is $H_s \approx 0.1H$, implying that the resultant mean wind speed is approximately $U(z)$ and the logarithmic law may be used for structural design purposes up to an elevation H_s; (5) at the top of the PBL $|V(H)| \approx 5u_*/k$ (Csanady 1967); and (6) as an artifact of the asymptotic method used to derive these results, at all other elevations $V(z)$ vanishes, that is, $V(z) = V(H)\delta(H)$, where $\delta(H)$ is the Dirac delta function (see Eq. 23, Appendix 1), a result that is physically unrealistic and is commented upon in Appendix 1.

Recently, computational fluid dynamics (CFD) has emerged as an approach that made possible the estimation of the variation of the component $V(z)$ with height. Equally importantly, it is now well established that the stratification of the free flow, the flow at elevations $z > H$, plays an important role in determining the characteristics of the PBL. According to Zilitinkevich and Esau (2002) and Zilitinkevich (2012), among others, neutrally-stratified flows can be either of the "truly neutral" or the "conventionally neutral" type. "Truly neutral" flows are characterized by a Kazanski–Monin surface buoyancy-flux parameter $\mu = 0$ and a non-dimensional number $\mu_N = N/|f| = 0$, where N is the Brunt–Väisäla frequency. Zilitinkevich et al. (2007) note that "truly neutral flows are observed during comparatively short transition periods after sunset on a background of residual layers of convective origin, … are often treated as irrelevant because of their transitional nature, and are usually excluded from data analysis;" "neutrally stratified PBLs are almost always conventionally neutral," that is, neutral *and* developing against a background stable stratification. They are characterized by $\mu = 0$, $\mu_N \neq 0$; typically $50 < \mu_N < 300$ (Zilitinkevich and Esau 2002; Zilitinkevich et al. 2007). Owing to strong mechanical (as opposed to thermal) turbulent mixing within the PBL, it is typically assumed for structural engineering purposes that, for strong winds, $\mu = 0$. For additional details, see Appendix 2.

The failure of the asymptotic similarity approach to consider stable stratification flow immediately above the PBL results in the incorrect prediction in realistic ("conventional") neutral barotropic PBL flows of height H, the cross-isobaric (veering) angle α_0 and its variation with height, and the geostrophic drag coefficient $C_g = u_*/G$, where G denotes the geostrophic wind speed. No current science-based information on the PBL is used at this time in tall-building design.

This note has three objectives: first, it recapitulates progress achieved in recent decades in the understanding and quantification of PBL characteristics of interest in tall-building design. Second, it presents a contribution to the development of criteria for such design. Last, but not least, it identifies the needs of tall-building designers so that improved design criteria can be developed.

2 Integral Measures of the Conventionally Neutral PBL

2.1 Geostrophic Drag Coefficient C_g and Cross-Isobaric Angle α_0

For Zilitinkevich numbers typical of conventionally neutral flows (i.e., $0.5 \times 10^2 < \mu_N < 3 \times 10^2$), the dependence of the geostrophic drag coefficient $C_g = u_*/G$ and the cross-isobaric angle α_0 upon the Rossby number $Ro = G/(|f|z_0)$ can be represented by the following expressions, based on measurements by Lettau (1962),

$$C_g = 0.205/(\log_{10} Ro - 0.556), \quad (1)$$

$$\alpha_0 = (173.58/\log_{10} Ro) - 3.03 \quad (2)$$

(Kung 1966; Hess and Garratt 2002 p. 338). Curves plotted in Fig. 2a, b of Zilitinkevich and Esau (2002) closely match Eqs. 1 and 2. As shown in the following example, the quantities G, C_g, and α_0 are obtained for any given u_*, f, and z_0 by using Eqs. 1 and 2.

Example 1 Assume $z_0 = 0.03$ m (open terrain exposure, see ASCE 7-10 2010), $u_* = 2.5\,\mathrm{m\,s^{-1}}$, $f = 10^{-4}\,\mathrm{s^{-1}}$. Since u_*, f, and z_0 are given, $C_g = u_*/G$, and $Ro = G/(|f|z_0)$, the only unknown in Eq. 1 is the geostrophic wind speed G. Equation 1 yields $G \approx 83\,\mathrm{m\,s^{-1}}$. Equation 2 then yields $\alpha_0 \approx 20°$.

2.2 PBL Height H

Zilitinkevich et al. (2007) proposed the following expression applicable to flows for which the Kazanski–Monin surface buoyancy flux parameter $\mu \approx 0$,

$$\frac{1}{H^2} = \left[\frac{f^2}{(C_R)^2} + \frac{N|f|}{(C_{CN})^2}\right]\frac{1}{u_*^2}, \quad (3)$$

where $C_R \approx 0.6$ and $C_{CN} \approx 1.36$. The non-dimensional form of H is

$$C_h(N, f) = Hf/u_*. \quad (4)$$

The application of Eqs. 3 and 4 is illustrated in the following example.

Example 2 For $u_* = 2.5\,\mathrm{m\,s^{-1}}$, $f = 10^{-4}\,\mathrm{s^{-1}}$ and $\mu_N = 100$ (i.e., $N = 0.01\,\mathrm{s^{-1}}$), Eq. 3 yields $H \approx 3300$ m and $C_h \approx 0.13$. In contrast, according to asymptotic estimates (e.g., Csanady 1967), $H \approx 0.25 \times 2.5/10^{-4} = 6250$ m (see Appendix 1, Eq. 9).

3 PBL Flows for Different Surface Roughness Regimes

Wind-speed fields are developed for structural engineering purposes under the assumption that the terrain has $z_0 \approx 0.03$ m over a sufficiently long fetch (i.e., that it corresponds in structural engineering terms to the category "open terrain exposure," see, e.g., Simiu and Scanlan 1996). Since structures commonly do not have "open terrain exposure," it is necessary to estimate, as functions of the surface roughness $z_{01} \neq z_0$, the friction velocity u_{*1} and the geostrophic height H_1 in a storm event that induces in terrain with open exposure a friction velocity u_*. Such estimates are based on the fact that, in large-scale storms, the geostrophic wind speed G is the same in both roughness regimes. Examples 3 and 4 consider, respectively, the cases of suburban and ocean versus open exposure.

Example 3 It was shown in the previous section that, given a surface with open exposure ($z_0 = 0.03$ m), with $f = 10^{-4}\,\mathrm{s}^{-1}$, to a storm that produces a friction velocity $u_* = 2.5\,\mathrm{m\,s}^{-1}$ there corresponds a geostrophic wind speed $G \approx 83\,\mathrm{m\,s}^{-1}$. In accordance with the definition of Ro, for suburban terrain exposure ($z_{01} = 0.3$ m over a sufficiently long fetch), to $G = 83\,\mathrm{m\,s}^{-1}$ there corresponds $\log_{10} Ro = \log_{10}[83/(10^{-4} \times 0.3)] = 6.44$. From Eq. 1, $C_\mathrm{g} = 0.035$, so $u_{*1} = 83 \times 0.035 \approx 2.9\,\mathrm{m\,s}^{-1}$, and the cross-isobaric angle is $\alpha_{01} \approx 24°$. From Eq. 3 there follows $C_{h1} = 0.13$ and $H_1 = 2.9 \times 0.13/10^{-4} \approx 3800$ m, vs. the asymptotic estimate $H = 7250$ m (Eq. 9).

Example 4 For ocean surfaces, assuming $G = 83\,\mathrm{m\,s}^{-1}$ and $z_0 = 0.003$ m, $\log_{10} Ro = \log_{10}[83/(10^{-4} \times 0.003)] = 8.44$, and $C_\mathrm{g} \approx 0.026$, so $u_{*1} = 83 \times 0.026 = 2.15\,\mathrm{m\,s}^{-1}$, and $\alpha_{01} \approx 18°$. It follows that $H_1 = 2800$ m and $C_\mathrm{h} = 0.13$ (vs. the asymptotic estimate $H = 5400$ m). Note that a structure built near the coastline and exposed to a wind direction from the ocean will be subjected to winds corresponding to ocean surface exposure.

The calculated heights H of the PBL are approximately half their counterparts obtained by using asymptotic methods, and an order of magnitude greater than their counterparts specified in the ASCE 7-10 and other standards on wind loads.

4 Effect of Veering on PBL Flow: A Case Study

Information on the variation with height z of the velocity components $U(z)$ and $V(z)$ (and therefore of their resultant) and of the angle $\alpha(z) = \tan^{-1}[V(z)/U(z)]$ is currently obtained from CFD simulations. We now consider a simulation reported in Hess (2004), in which the coefficient C_h and the height H are denoted by h_* and z_i, respectively (see Eq. 27, p. 320, and p. 321 therein), and $C_\mathrm{h} \equiv h_* = 0.10$. Figures 1 and 2 show the dependence on height z of $U(z)$ and $V(z)$, of their resultant, and of the angle $\alpha(z)$, as represented in Fig. 6 of Hess (2004).

Example 5 Consider the following parameters: $f = 10^{-4}\,\mathrm{s}^{-1}$, $N = 0.018\,\mathrm{s}^{-1}$, so $\mu_N = 180$, and $z_0 = 0.3$ m, $u_* = 1.5\,\mathrm{m\,s}^{-1}$. It can be verified by using Eq. 3 that $C_\mathrm{h} \approx 0.10$, so $H = 0.10 \times 1.5/10^{-4} = 1500$ m. Further, the value $G = 41\,\mathrm{m\,s}^{-1}$ yields $\log_{10}(Ro) = 6.14$, $u_*/G \approx 0.037$, to which corresponds $G = 41\,\mathrm{m\,s}^{-1}$, and $\alpha_0 \approx 25°$. For $z = 300$ m, $z/H = 0.20$, and for $z = 800$ m, $z/H = 0.53$. Figure 1 shows that the component V (800 m) and, a fortiori, the component V (300 m), have negligible contributions to the resultant mean wind speed, and that the veering angles α (300 m) and α (800 m) are approximately 2° and 6°, respectively. Results for $C_\mathrm{h} = 0.19$, based on Fig. 7 of Hess (2004), are also included in Figs. 1 and 2.

5 Conclusions

Numerical results obtained for cases of interest for tall structure design and believed to be reasonably representative suggest that:

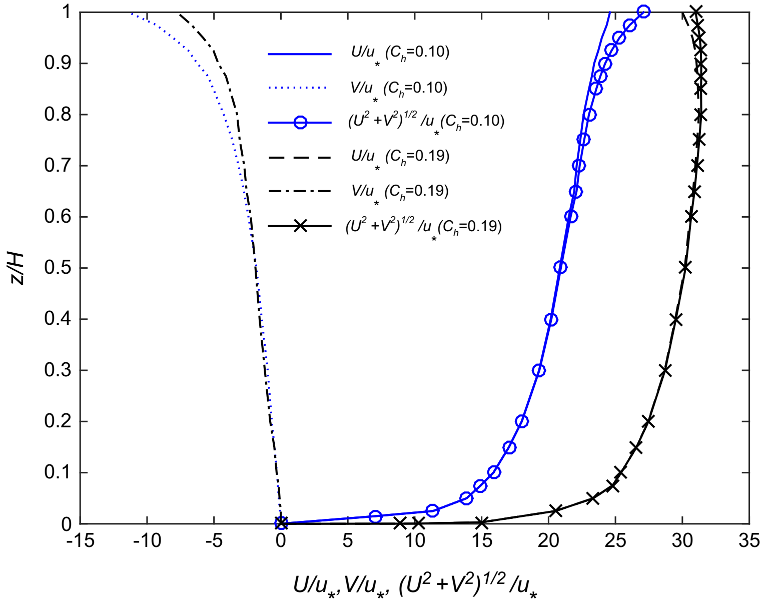

Fig. 1 Dependence of U/u_*, V/u_*, and $\sqrt{U^2 + V^2}/u_*$ on z/H

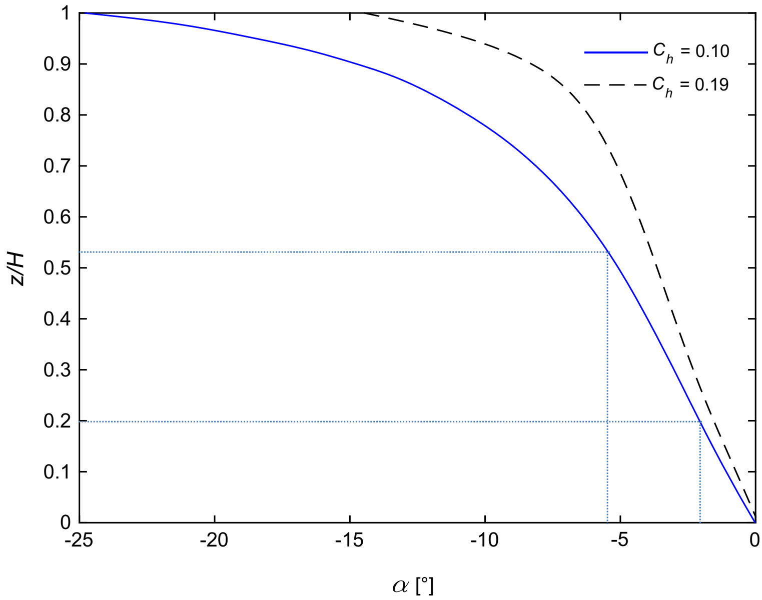

Fig. 2 Dependence of veering angle α on z/H

1. Mean wind speeds increase monotonically with height up to considerably higher elevations than those inherent in power-law models specified by current codes and standards. This can affect the design of structures with heights greater than the gradient heights specified in the ASCE 7-10 and other standards on wind loads.

2. The contribution to the resultant mean wind speed of the component $V(z)$ normal to the surface stress is negligible for elevations of the order of, say, 1 km and lower.
3. The veering angle was found to be small (e.g., approximately 2° and 6° for 300 m and 800 m elevations z, respectively).
4. Given a storm with winds characterized by the friction velocity u_* at a location with surface roughness z_0, simple calculations allow the estimation of the friction velocity induced by the same storm at a nearby location where the surface roughness differs from z_0.

Numerical examples presented herein illustrate these points. In the authors' view efforts to improve current tall-building structural design practices would benefit from the dialogue this note attempts to initiate between PBL meteorologists and structural engineers.

Acknowledgments The authors wish to express their appreciation to the reviewers for their thorough review and helpful comments.

Appendix 1: Mean Velocity Field Model Based on Classical Asymptotic Approach

The purpose of this Appendix is to show that the asymptotic approach yields a physically unrealistic representation of the variation of the velocity component V with height.

The starting point of the asymptotic approach is the partitioning of the neutral boundary layer into two regions, an (inner) surface layer and an outer layer. In the surface layer the shear stress τ_0 induced by the boundary-layer flow at the Earth's surface must depend upon the flow velocity at a distance z from the surface, the roughness length z_0, and the density ρ of the air, that is,

$$\tau_0 \mathbf{i} = F\left(U\mathbf{i} + V\mathbf{j}, z, z_0, \rho\right), \tag{5}$$

where U and V are the components of the mean wind velocity along the x and y directions and $\mathbf{i}$, $\mathbf{j}$ are unit vectors. Equation 5 can be written in non-dimensional form

$$\frac{U\mathbf{i} + V\mathbf{j}}{u_*} = \psi_{1x}\left(\frac{z}{z_0}\right)\mathbf{i} + \psi_{1y}\left(\frac{z}{z_0}\right)\mathbf{j}, \tag{6}$$

where

$$u_* = \left(\frac{\tau_0}{\rho}\right)^{1/2} \tag{7}$$

is the friction velocity and $\boldsymbol{\Psi}_1 = \Psi_{1x}\mathbf{i} + \Psi_{1y}\mathbf{j}$ is a vector function to be determined. Equation 6 is known as the *law of the wall*, which is applicable in the surface layer, and can be written in the form

$$\frac{U\mathbf{i} + V\mathbf{j}}{u_*} = \psi_{1x}\left(\frac{z}{H}\frac{H}{z_0}\right)\mathbf{i} + \psi_{1y}\left(\frac{z}{H}\frac{H}{z_0}\right)\mathbf{j}, \tag{8}$$

where

$$H = cu_*/f, \tag{9}$$

and H denotes the boundary-layer depth, and on the basis of data available in the 1960s it was assumed in Csanady (1967) $c \approx 0.25$.

The mean velocity components $U(H)$ and $V(H)$ are denoted by U_{g} and V_{g}, respectively. Their resultant, denoted by G, is the magnitude of the geostrophic velocity. In the outer layer it can be asserted that, at height z, the velocity reduction with respect to G must depend upon the surface shear stress τ_0, and the air density ρ. The expression for this dependence in non-dimensional form is known as the *velocity defect law*,

$$\frac{U\mathbf{i}+V\mathbf{j}}{u_*}=\frac{U_{\mathrm{g}}\mathbf{i}+V_{\mathrm{g}}\mathbf{j}}{u_*}+\psi_{2x}\left(\frac{z}{H}\right)\mathbf{i}+\psi_{2y}\left(\frac{z}{H}\right)\mathbf{j}, \tag{10}$$

where $\mathbf{\Psi}_2$ is a vector function to be determined.

Consider, in Eqs. 6 and 10, the x components

$$\frac{U\mathbf{i}}{u_*}=\psi_{1x}\left(\frac{z}{H}\frac{H}{z_0}\right)\mathbf{i}, \tag{11}$$

$$\frac{U\mathbf{i}}{u_*}=\frac{U_{\mathrm{g}}\mathbf{i}}{u_*}+\psi_{2x}\left(\frac{z}{H}\right)\mathbf{i}. \tag{12}$$

From the observation that a multiplying factor inside the function Ψ_{1x} must be equivalent to an additive function outside the function Ψ_{2x} the following are obtained,

$$\frac{U}{u_*}=\frac{1}{k}\left(\ln\frac{z}{h}+\ln\frac{H}{z_0}\right), \tag{13}$$

$$\frac{U}{u_*}=\frac{U_{\mathrm{g}}}{u_*}+\frac{1}{k}\left(\ln\frac{z}{h}\right), \tag{14}$$

for the surface layer and the outer layer, respectively. From Eq. 13 it follows immediately

$$\frac{U}{u_*}=\frac{1}{k}\ln\left(\frac{z}{z_0}\right). \tag{15}$$

By equating Eqs. 13 and 14 in the overlap region there results

$$\frac{U_{\mathrm{g}}}{u_*}=\frac{1}{k}\ln\left(\frac{H}{z_0}\right). \tag{16}$$

The logarithmic law is seen to apply to the U component of the wind velocity throughout the depth of the boundary layer.

Consider now the components

$$\frac{V\mathbf{j}}{u_*}=\psi_{1y}\left(\frac{z}{H}\frac{H}{z_0}\right)\mathbf{j}, \tag{17}$$

$$\frac{V\mathbf{j}}{u_*}=\frac{V_{\mathrm{g}}\mathbf{j}}{u_*}+\psi_{2y}\left(\frac{z}{H}\right)\mathbf{j} \tag{18}$$

Csanady (1967), Blackadar and Tennekes (1968) and Tennekes (1973) assume $\Psi_{1y}\equiv 0$. Then, Eqs. 17 and 18 yield, in the overlap region,

$$\frac{V_{\mathrm{g}}}{u_*}+\psi_{2y}\left(\frac{z}{H}\right)=0, \tag{19}$$

that is,

$$\psi_{2y}\left(\frac{z}{H}\right)=-\frac{V_{\mathrm{g}}}{u_*}, \tag{20a}$$

$$\psi_{2y}\left(\frac{z}{H}\right)=\frac{B}{k}, \tag{20b}$$

where, based on measurements available in the 1960s, it is assumed $B/k \approx 12$ (e.g., Csanady 1967). It follows from Eqs. 18 and 20a that

$$V(z) = 0 \qquad (z < H). \tag{21}$$

Since, for $z = H$, $V(H) = V_g$, Eq. 18 yields

$$\Psi_{2y}(H/H) = 0 \quad (z = H), \tag{22}$$

and, by virtue of Eqs. 19 and 21,

$$V(z) = V_g \delta(H), \tag{23}$$

where δ denotes the Dirac delta function. This physically unrealistic result is an artifact of the asymptotic approach, which transforms the actual profile $V(z)$ (of which two CFD-based estimates are represented in Fig. 1) into the non-physical profile represented by Eq. 23.

Appendix 2: Brunt–Väisäla Frequency and 'Conventionally Neutral' PBL Flow

According to research results cited by, among others, Zilitinkevich et al. (2007), the stratification, characterized by the free-flow Brunt–Väisäla frequency N, has a significant effect on the PBL. Based on the dependence of PBL flow upon both the buoyancy flux μ at the Earth's surface and the free-flow Brunt–Väisäla frequency N, Zilitinkevich et al. (2007) classify neutral and stable PBL flows into four categories: (i) "truly neutral" ($\mu = 0, N = 0$); (ii) "conventionally neutral" ($\mu = 0, N > 0$), (iii) "short-lived stable," ($\mu < 0, N = 0$), and (iv) "long-lived stable" ($\mu < 0, N > 0$). Of these four categories it is the "conventionally neutral" flow that is, in practice, of interest in structural engineering applications.

An air parcel moving vertically is subjected to a gravitational force due to the variation of the air density with height, and the differential equation describing the vertical motion of the air parcel has an oscillatory solution. In the presence of a horizontal flow, the vertical oscillations result in a transport of momentum between the free flow and the PBL flow. As a result of this transport the PBL flow velocities are increased, thus causing a reduction in the height of the PBL with respect to the height of the "truly neutral" PBL. The decrease of the height H as N (i.e., the strength of the stratification) increases is reflected in Eq. 3.

References

AIJ recommendations for Loads on Buildings (2004) Chapter 6. Architectural Institute of Japan, 81 pp. http://www.aij.or.jp/jpn/symposium/2006/loads/loads.htm. Accessed 5 Jun 2015

ASCE 7-10 Standard (2010) Minimum design loads for buildings and other structures. American Society of Civil Engineers, Reston, 608 pp

Blackadar AK, Tennekes H (1968) Asymptotic similarity in neutral barotropic planetary boundary layer. J Atmos Sci 25:2015–2020

Canadian Structural Design Manual (1971) Supplement No. 4 to the National Building Code of Canada. National Research Council of Canada, Ontario, 380 pp

Csanady GT (1967) On the 'resistance law' of a turbulent Ekman layer. J Atmos Sci 24:467–471

Davenport AG (1965) The relationship of wind structure to wind loading. In: Symposium on wind effects on buildings and structures, vol 1. National Physical Laboratory, Teddington, Her Majesty's Stationery Office, London, pp 53–102

Hess GD (2004) The neutral barotropic planetary boundary layer, capped by a low-level inversion. Boundary-Layer Meteorol 110:339–355

Hess GD, Garratt JR (2002) Evaluating models of the neutral, barotropic planetary boundary layer using integral measures: Part I. Overview. Boundary-Layer Meteorol 104:333–358

Kung EC (1966) Large-scale balance of kinetic energy in the atmosphere. Mon Weather Rev 94:627–640

Lettau HH (1962) Theoretical wind spirals in the boundary layer of a barotropic atmosphere. Beitr Phys Atmos 35:195–212

Simiu E, Scanlan RH (1996) Wind effects on structures, 3rd edn. Wiley, Hoboken, 688 pp

Tennekes H (1973) The logarithmic wind profile. J Atmos Sci 30:234–238

Zilitinkevich SS (2012) The height of the atmospheric planetary boundary layer: state of the art and new development. In: Fernando H et al (eds), National security and human health implications of climate change. NATO science for peace and security series C: Environmental Security. Springer. doi:10.1007/978-04-007-2430-3_13

Zilitinkevich SS, Esau I (2002) On integral measures of the neutral barotropic planetary boundary layer. Boundary-Layer Meteorol 104:371–379

Zilitinkevich SS, Esau I, Baklanov A (2007) Notes and correspondence: further comments on the equilibrium height of neutral and stable planetary boundary layers. Q J R Meteorol Soc 133:265–271